Conf-920311--19

GA-A--20904

DE92 016249

BORONIZATION IN DIII–D

by
G.L. JACKSON, J. WINTER, K.H. BURRELL, J.C. DeBOO,
C.M. GREENFIELD, R.J. GROEBNER, T. HODAPP,
A.G. KELLMAN, R. LEE, S.I. LIPPMAN, R. MOYER,
J. PHILLIPS, T.S. TAYLOR, J. WATKINS, and W.P. WEST

MAY 1992

GENERAL ATOMICS

DISCLAIMER

GA–A20904

BORONIZATION IN DIII–D

by

G.L. JACKSON, J. WINTER,* K.H. BURRELL, J.C. DeBOO, C.M. GREENFIELD, R.J. GROEBNER, T. HODAPP, A.G. KELLMAN, R. LEE, S.I. LIPPMAN, R. MOYER,† J. PHILLIPS, T.S. TAYLOR, J. WATKINS,‡ and W.P. WEST

This is a preprint of a paper to be presented at the 10th International Conference on Plasma Surface Interactions, March 30 through April 3, 1992, Monterey, California, and to be printed in the *Proceedings.*

Work supported by
U.S. Department of Energy
Contract No. DE-AC03-89ER51114

* Institute of Plasmaphysics, KFA, Jülich, FRG.
† University of California at Los Angeles.
‡ Sandia National Laboratories, Livermore, California.

GENERAL ATOMICS PROJECT 3466
MAY 1992

GENERAL ATOMICS

ABSTRACT

A thin boron film has been applied to the DIII–D tokamak plasma facing surfaces to reduce impurity influx, particularly oxygen and carbon. A direct result of this surface modification was the observation of a regime of very high energy confinement, VH–mode, with confinement times from 1.5 to 2 times greater than predicted by the H–mode scaling relation for the same set of parameters. VH–mode discharges are characterized by low ohmic target densities, low edge neutral pressure, and reduced recycling. These conditions have reduced the collisionality, ν^*, in the edge region producing a higher edge pressure gradient and a significant bootstrap current, up to 30% of the total current.

We will describe the edge plasma properties after boronization including reductions in recycling inferred from measurements of τ_p^*. In particular we will discuss the edge plasma conditions necessary for access to VH–mode including the boronization process and properties of the deposited film.

1. INTRODUCTION

Boronization has been applied to the DIII–D tokamak to reduce the influx of oxygen impurities and to lower the fraction of radiated power. Boronization is a chemical vapor deposition process (CVD) which produces a thin boron film (~100 nm average thickness) on all plasma facing surfaces using a glow discharge and a mixture of helium (90%) and diborane (10%) gases. Boronization was applied in the TEXTOR tokamak in 1988 [1] and the process used in DIII–D is based upon the TEXTOR system [2,3].

After boronization in DIII–D oxygen, carbon, and nickel impurities were substantially reduced during tokamak discharges allowing operation with lower radiated power and lower $Z_{\rm eff}$. A direct consequence of this wall conditioning technique was the attainment of a new enhanced confinement regime. This regime of very high confinement is referred to as VH–mode [4]. It has been obtained in post-boronization double-null diverted discharges and is characterized by low edge neutral pressure, a low fraction of radiated power (typically <30% for 1.6 MA discharges), a high calculated bootstrap current in the edge region, and a steadily increasing energy confinement time. Energy confinement times up to a factor of 3.5 above ITER 89-P L–mode scaling [5] and a factor of 1.5 to 2 above previous DIII–D/JET [6] scaling have been observed.

In this paper we will first describe the boronization process used in DIII–D including techniques to produce a more uniform boron coating. We next discuss the effect of boronization on tokamak discharges and in particular the VH–mode. The effect of the boron film on recycling and particle influx is also presented.

2. THE DIII-D BORONIZATION PROCESS

The purpose of boronization in DIII–D is to reduce oxygen and cover all plasma facing surfaces with a low Z film. The DIII–D plasma facing surfaces are primarily Inconel (60%) and graphite (40%). Although graphite has been installed in areas which are routinely exposed to the highest heat fluxes, pre-boronization high current ($I_p \geq 1.5$ MA) beam-heated H–mode discharges have shown nickel impurity accumulation. The DIII–D boronization system is shown in Fig. 1. Initially only one gas injection port was installed but residual gas analysis (RGA) and surface samples showed that the boron film had a significant toroidal non-uniformity. The toroidal nonuniformity of the boron film is caused by the high sticking efficiency of the diborane molecule and its dissociated particles [7]. After the first boronization, another gas injection point was added to improve toroidal uniformity and provide a thicker boron film near the ion cyclotron heating (ICH) rf antenna. RGA spectra are shown in Fig. 2 during the boronization process with (a) the glow discharge on and (b) the glow discharge off (gas flow only). There is a large, factor of $\sim$15, decrease in the diborane partial pressure measured at the RGA during the glow discharge when compared to gas flow only. Note that the RGA does not detect diborane, B_2D_6 which is $m/e = 34$. The diborane molecule is easily dissociated and in this paper we will use mass 32, B_2D_5 as an indication of the diborane partial pressure. The RGA is located 2.4 m and 7.4 m toroidally from the gas injection ports and these spectra were taken with equal rates of gas flow from both ports.

To further improve toroidal uniformity a pulsed glow discharge was implemented. During the low current phase of the pulsed glow discharge, typically $I_{glow} = 0.5$ amperes for 2 s, the diborane partial pressure nearly equilibrates around the torus and the neutral density of diborane increases. During the high current phase, typically $I_{glow} = 5$ amperes for 1 s, the diborane is deposited more uniformly around the torus by the higher glow current. The RGA partial pressure of $m/e = 32$, B_2D_5, is shown in Fig. 3 as a function of

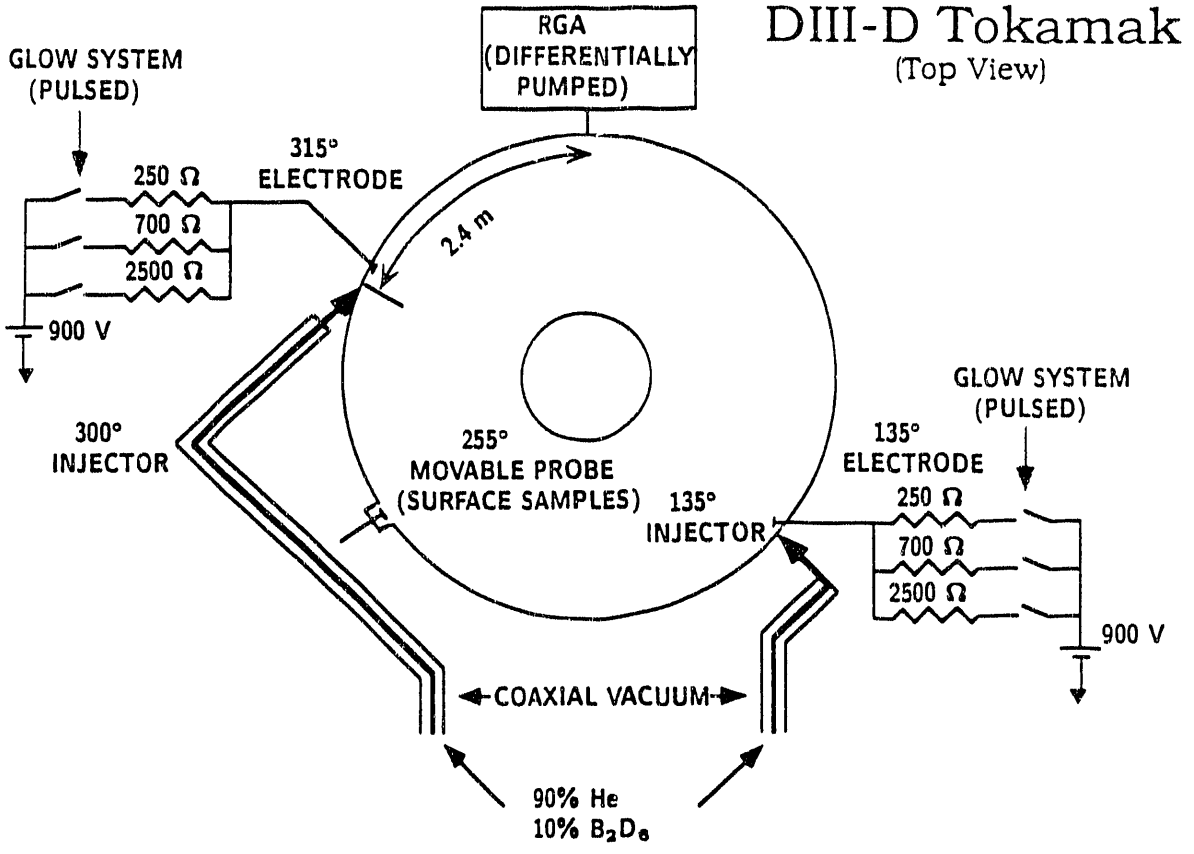

Fig. 1. Schematic representation of the DIII–D boronization injection and glow discharge systems. The pumping system is not shown. The gas injector and electrode which are located at 135° toroidally are separated vertically by ~1 m.

the average current, $I_{av} = 5xDF + 0.5x(1 - DF)$, where DF is the duty factor (a gas flow only point, $I_{av} = 0$, is also included in Fig. 3). Note that the diborane partial pressure is an exponential function of the average current, shown as a dashed line in Fig. 3. We have chosen to operate at a DF of ~1/3 resulting in a reduction of the RGA mass 32 signal by a factor of ~4 as a compromise between uniformity and efficient use of diborane.

After the installation of the second diborane injection port and implementation of the pulsed glow discharge the film thickness, measured by surface samples at the location shown in Fig. 1, has increased by a factor of ~3 when compared to the first boronization session [3].

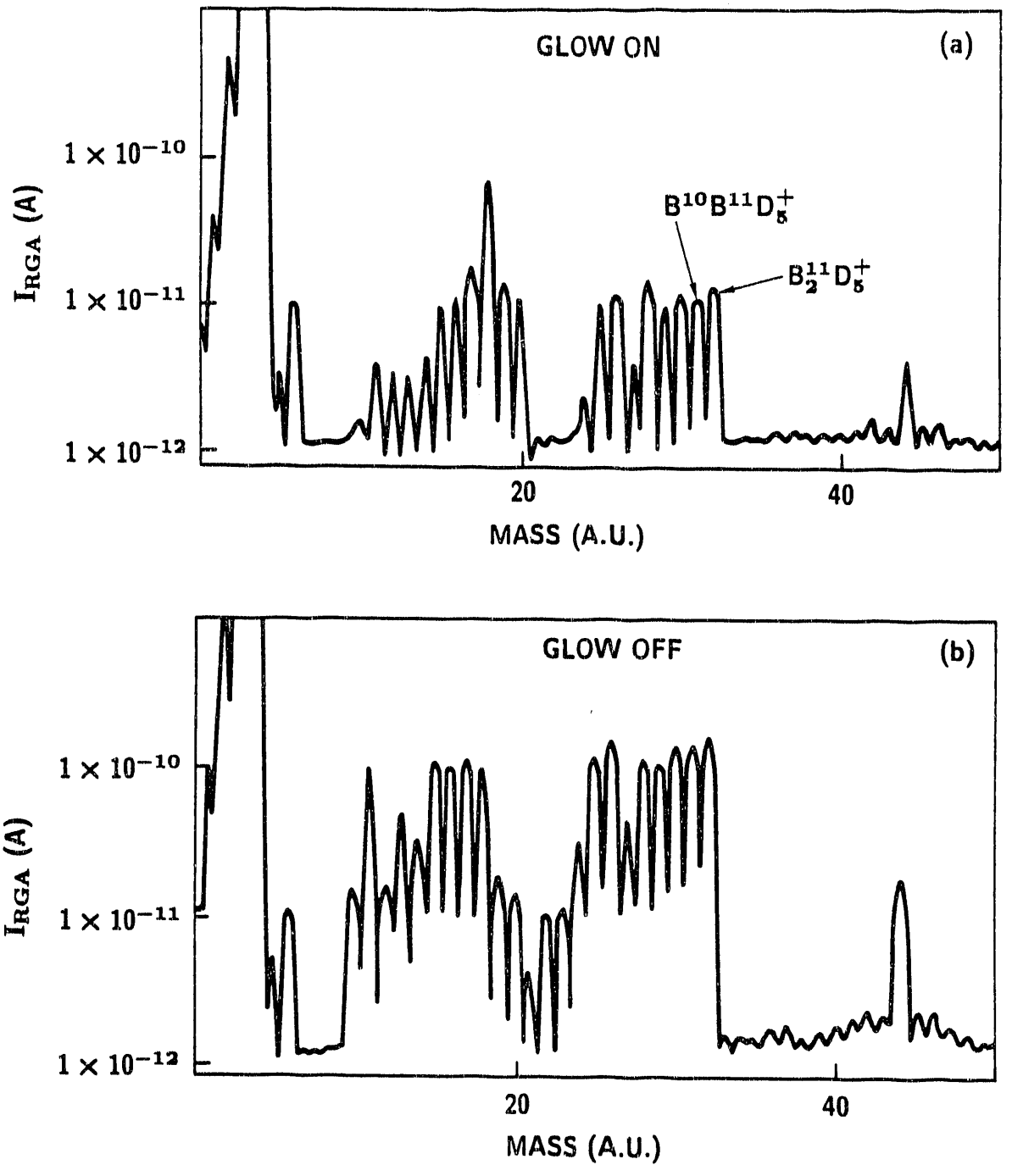

Fig. 2. Diborane partial pressure is reduced by a factor of ~15 during a boronization (a) glow discharge, $I_{glow} = 5$ A, when compared to (b) no glow discharge at the same gas flow rate. Both B^{10} and B^{11} are observed in the approximate ratio of their natural composition. The RGA scale is "quasilinear".

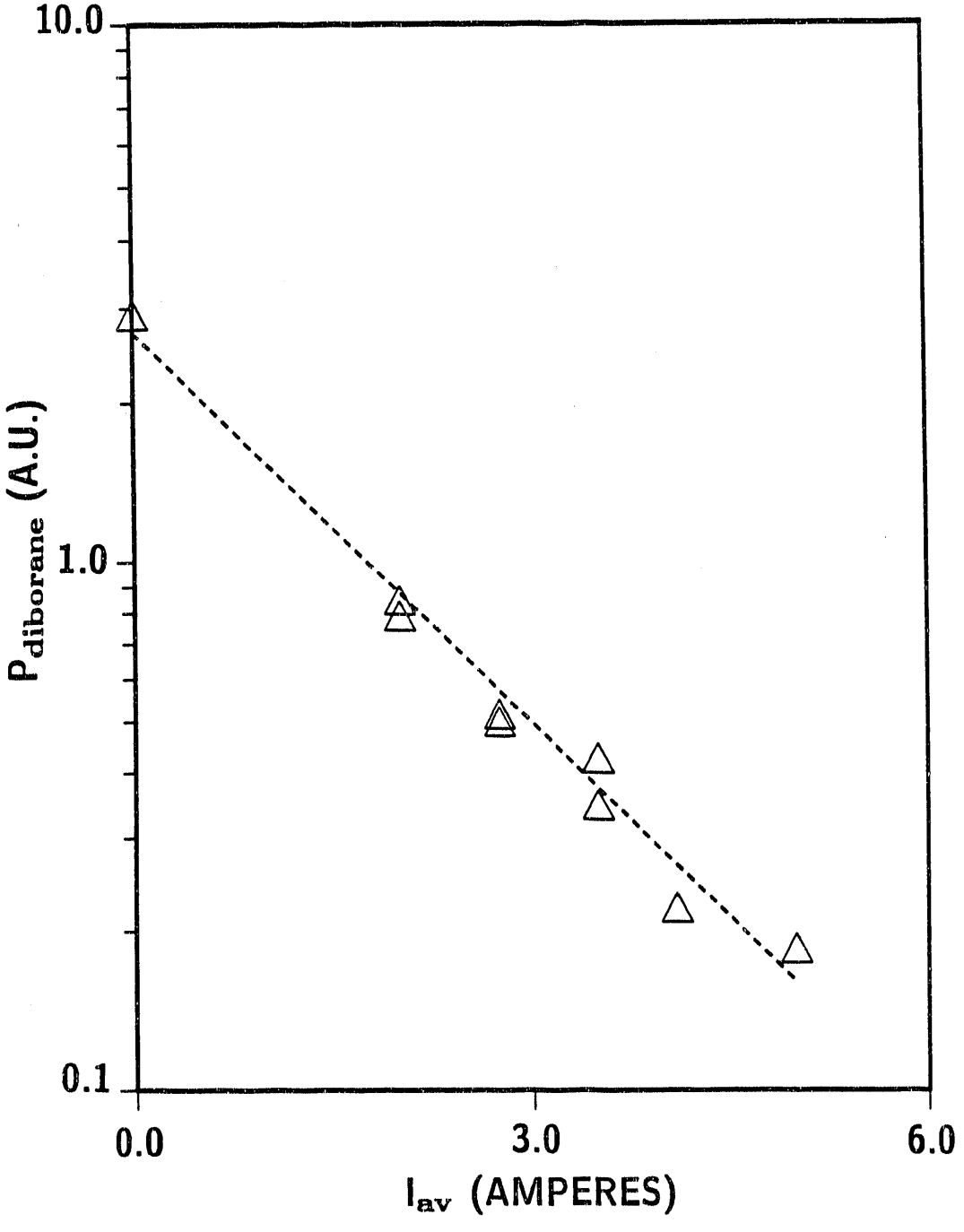

Fig. 3. The partial pressure of diborane inferred from B_2D_5 decreases exponentially during a pulsed glow as the average current increases. $I_{glow}^{high} = 5$ amperes and $I_{glow}^{low} = 0.5$ amperes. The RGA location with respect to the injector positions is shown in Fig. 1.

The first evidence of changes in wall condition following boronization was significant reductions in impurity gases evolved during baking. DIII–D normally operates with room temperature walls but the vessel is periodically baked, $T_{av} \leq 400\,^{\circ}C$. When two baking sessions are compared, one before and one after boronization, all residual gases are reduced after boronization and the partial pressures of oxygen containing gases, (D_2O, CO, CO_2), are all reduced by more than one order of magnitude.

3. POST-BORONIZATION TOKAMAK DISCHARGES

Post-boronization tokamak discharges showed reductions in impurity line radiation of oxygen, carbon and nickel by factors of 3–5, ~2, and 10–30 respectively when compared to similar tokamak discharges before boronization [3,8]. Both before and after boronization, boron impurity line radiation, measured by the SPRED U-V spectrometer, was not a significant contribution to either $Z_{\rm eff}$ or radiated power. Prior to boronization in DIII–D, carbonization has reduced nickel impurity line radiation and also, transiently, oxygen radiation [9] with little or no increase in carbon impurities. However boronization has reduced the levels of O, C, and Ni to the lowest values yet obtained [10].

With reduced impurity influxes and reduced particle fueling which is discussed in the next section, low ohmic target density discharges were obtained with lower $Z_{\rm eff}$ and lower radiated power than was possible before boronization. A direct consequence of this operation was the achievement of a new regime of very high confinement, VH–mode. VH–mode is characterized by thermal energy confinement 1.5 to 2 times above the previous DIII–D/JET H–mode empirical scaling relation [6].

Another characteristic of VH–mode is the low fraction of radiated power, <30%. A general feature of these VH–mode mode discharges is that there is little or no central impurity accumulation. This behavior is distinct from previous high current ELM-free *H–mode* discharges where impurity line radiation, particularly nickel, continued to increase throughout the quiescent H–mode phase. Nickel is the main component of the DIII–D Inconel walls and 60% of the plasma facing surface is Inconel.

In conjunction with the lower particle fueling and lower target density after boronization, the edge collisionality, ν^*, is reduced and edge temperature and pressure gradients are high, as shown in Fig. 4. Low collisionality produces a substantial calculated bootstrap current and reduced edge magnetic shear. With the strong shaping produced by a double-null configuration and the low edge shear, the outer region from $0.85 \lesssim \rho \lesssim 1.0$ of

post-boronization VH–mode discharges is calculated to be in the second stable region to ideal ballooning modes [11].

The reduced edge collisionality can also cause changes in the plasma rotation and the electric field profile. An inward shift in the region of the highest electric field gradient is observed during VH–mode [11] and may also account for the confinement improvement.

The electron density, temperature, and pressure, and the ion temperature profiles during the VH–mode phase are shown in Fig. 4. There is a broad region, $0.8 < \rho < 1.0$, where the electron pressure decays exponentially as a function of the normalized radius, ρ. The radial extent over which this exponential decay is observed is larger than in H–mode discharges.

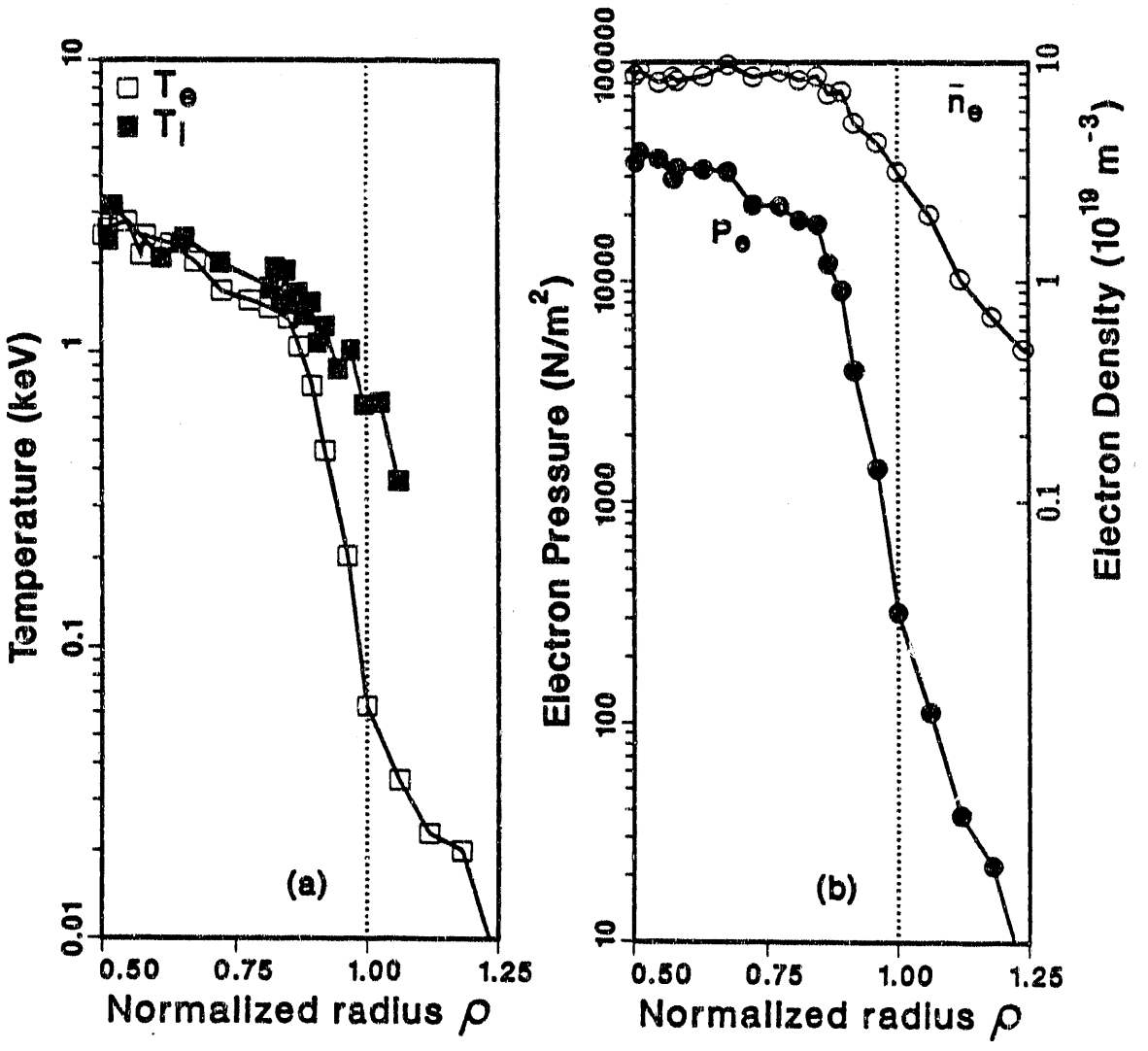

Fig. 4. Electron and ion temperature, electron density, and electron pressure profiles during the VH–mode phase of a post-boronization discharge (#73290) for $\rho > 0.5$. The last closed flux surface is shown as a dashed line.

4. PARTICLE FUELING

Particle fueling from plasma facing surfaces is reduced after boronization. It should be noted that nearly all DIII–D tokamak discharges are preceded by a short session of helium glow wall conditioning (HeGWC) to reduce particle fueling from the walls [12]. A comparison of particle fueling after boronization accompanied by HeGWC and pre-boronization HeGWC only is shown in Fig. 5. In this figure, the initial rate of particle influx, $dN(0)/dt$, is measured by the electron density rise at the start of neutral beam heating. The initial rate of particle change $dN(0)/dt$ is normalized to the neutral beam particle flux, $\Gamma_{\mathbf{beam}}$. For no wall fueling, $(dN_e(0)/dt)/\Gamma_{\mathbf{beam}}$ would be unity. Using a least squares fit, the number of plasma particles can expressed as [10]

$$N_D(t) = (\Gamma_{\mathbf{beam}} + \Gamma_{\mathbf{wall}})\ \tau_p^* + \left[N_{eo} - (\Gamma_{\mathbf{beam}} + \Gamma_{\mathbf{wall}})\ \tau_p^*\right]\ e^{-t/\tau_p^*} \qquad (1)$$

where $N_D = \bar{n}_e \times V_p$, $Z_{\mathbf{eff}}$ is assumed constant and equal to unity for this simple model. V_p is the plasma volume and $\bar{n}_e$ is the average electron density inferred from I-R interferometry and magnetic equilibria. $\tau_p^* = \tau_p/(1\text{-}R)$, τ_p is the global particle confinement time and R is the global recycling coefficient. $\Gamma_{\mathbf{wall}}$ is a wall fueling term and N_{eo}, τ_p^* and $\Gamma_{\mathbf{wall}}$ are fitting parameters assumed constant in time during the fitting interval.

As shown in Fig. 5, boronization accompanied by HeGWC substantially reduces the ratio, $(dN_e(0)/dt)/\Gamma_{\mathbf{beam}}$. During the beam heated phase of these discharges when this ratio is calculated there is no external gas fueling, and the only external particle fueling was neutral beam particles.

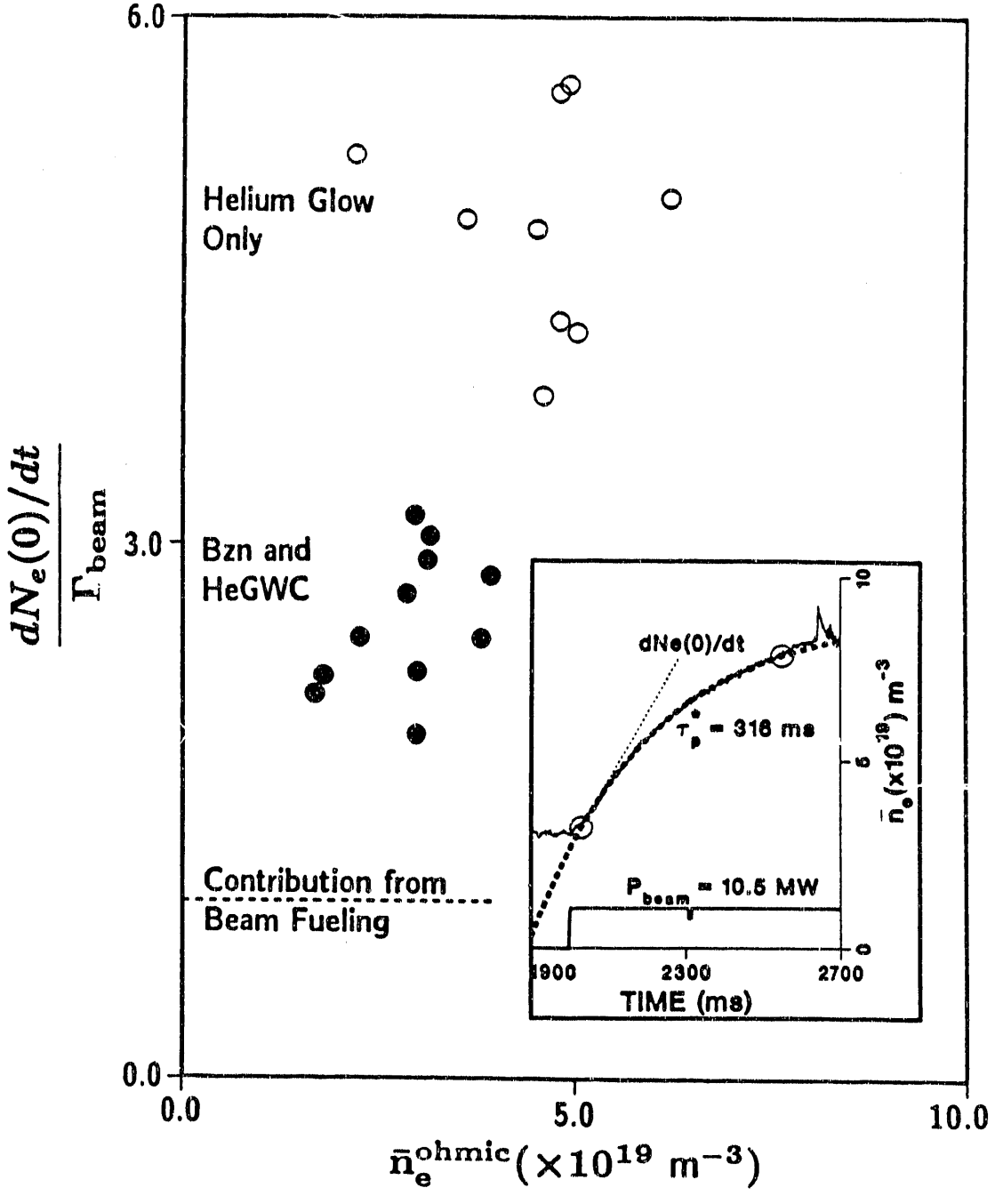

Fig. 5. Wall fueling is reduced after boronization for beam-heated discharges. The ratio of the initial rate of rise of the total number of electrons to the number of beam particles is plotted. $dN_e(0)/dt$ (dotted line) is inferred from a least squares fit to the electron density (dashed line in inset). The plasma volume is calculated from the magnetic equilibria. The range of the fit is shown by open circles. Discharge parameters: 1-2 MA, $D^\circ \rightarrow D^+$ at 3 to 16 MW, 2 T , lower single-null and double-null diverted discharges.

As discussed above, the recycling particle confinement time, τ_p^*, can be inferred from the density rise after a sudden change in either the confinement time (L–mode to H– or VH–mode), or a change in the external particle fueling, *i.e.* a change in neutral beam heating power. τ_p^* is shown in Fig. 6 both for VH–mode discharges and for previous H–mode discharges. Note that as the ohmic electron target density increases, τ_p^* decreases for both VH–mode and H–mode discharges.

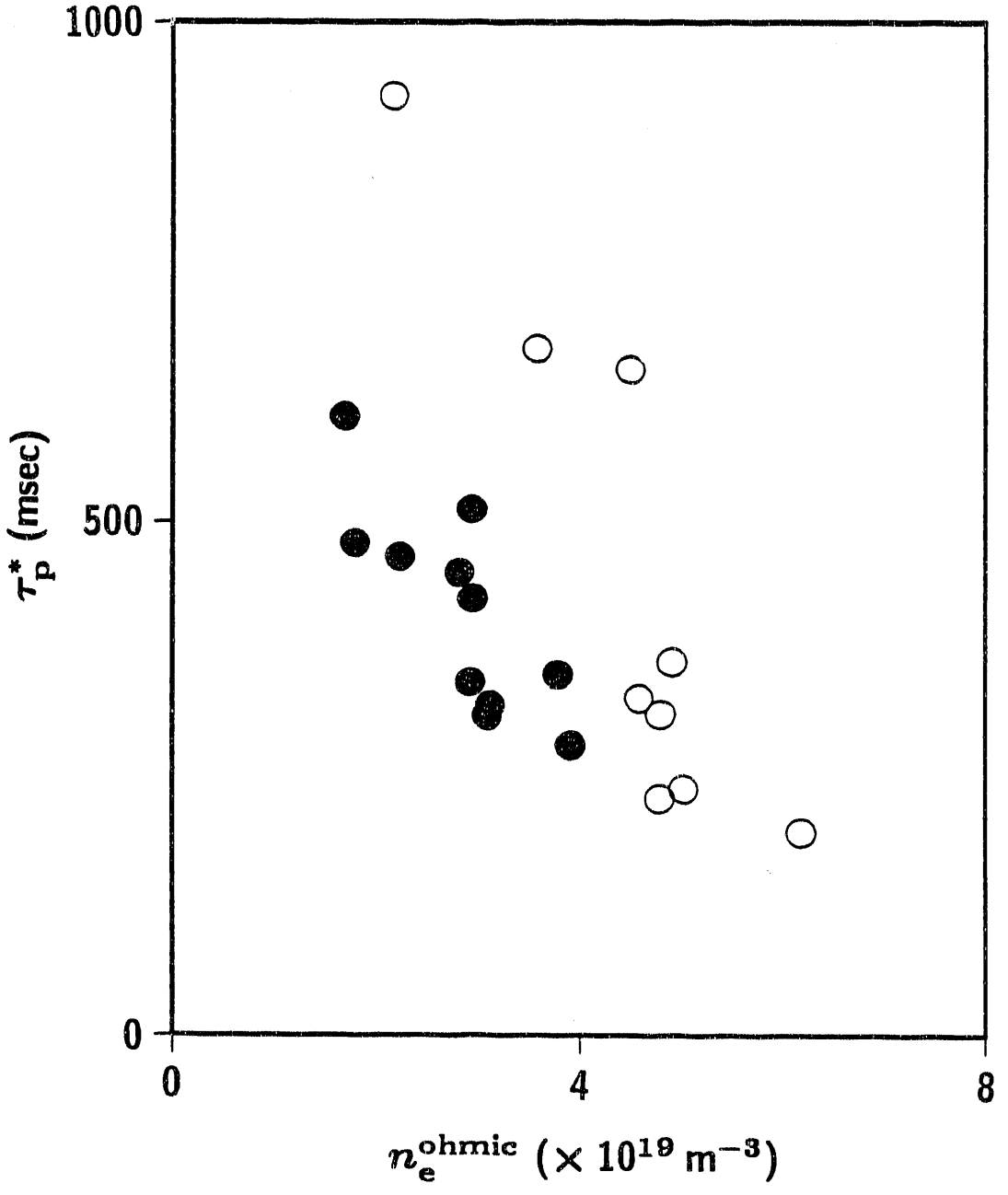

Fig. 6. The global particle recycling confinement time, τ_p^*,inferred from an exponential fit during the ELM-free density rise in VH-mode (•) or H-mode (○) phase of the discharge. For similar values of ohmic target density, τ_p^* is lower after boronization.

5. DISCUSSION

Boronization accompanied by HeGWC has reduced radiated power and impurity influx to the lowest values for comparable tokamak discharges of all wall conditioning techniques used so far in DIII–D [10]. After boronization the operating regime of DIII–D allowed operation at lower ohmic target densities with lower Z_{eff} and radiated power than was previously possible and this produced a new regime of very high confinement, VH–mode.

The intial boronization was very nonuniform. The scale length of this nonuniformity can be estimated from Fig. 2 assuming that the deposition rate for the boron film, R_B, is proportional to the density of diborane molecules which in turn is proportional to the measured partial pressure, *i.e.* $R_B \propto e^{-x/L_B}$, where x is the distance from the gas injection port and L_B is the characteristic scale length. From Fig. 2 we estimate the $L_B \sim 0.9$ m for $I_{glow} = 5$ amperes, which is consistent with observations from the TEXTOR tokamak [7]. Assuming that the local deposition rate is also proportional to the glow current density (assumed toroidally constant since the gas mixture consists of 90% helium), L_B is inversely proportional to the average glow current and the partial pressure is predicted to show an exponential decrease as a function of I_{glow}. This exponential behavior is observed experimentally and is plotted in Fig. 3. The implementation of a second diborane injection port and the pulsed glow discharge has improved the toroidal uniformity of the boron film.

Boronization has an additional benefit of reducing wall fueling, which has also been observed in other machines [1]. Even during neutral beam heating there is a reduction in wall fueling. We speculate that the reduced wall fueling is a combination of several factors: less physical desorption of deuterium by oxygen and carbon sputtering, the use of HeGWC before the tokamak discharge, and the ability of the boron film, when compared to graphite, to more effectively bind deuterium.

There is a decrease in τ_p^* after boronization for discharges with the same target density, shown in Fig. 6. This is consistent with lower recycling, but we cannot exclude the possibility that the global particle confinement time, τ_p, has also changed. Further experiments are required to separate the effect of R and τ_p.

The decrease of τ_p^* in Fig. 6 as ohmic target density increases is somewhat surprising. One would expect that as the density increases, the walls become saturated, the recycling coefficient (R) increases, and hence τ_p^* increases. A possible explanation is that higher target density increases transport in the SOL and outer plasma region, lowering the particle confinement time so that this effect dominates during the H–mode and VH–mode phases shown in Fig. 6. An alternative explanation for this observation is that higher target density results in a thicker denser SOL and decreases penetration of neutrals to the separatrix, thus decreasing the effective recycling coefficient. Further experiments and edge plasma modeling are planned investigate this.

Boronization has provided a clear example of the importance of plasma surface interactions in determining overall plasma performance. The addition of this wall conditioning technique in DIII–D produced a new confinement regime, VH–mode, and increased the highest triple product, $n_i T_i \tau_E$, obtained in DIII–D, by a factor of two, to 2.0×10^{20} s keV m^{-3}. The boron film was sufficient to achieve VH–mode at any time during an experimental campaign extending for 6 days and 150 discharges. While oxygen was substantially reduced after boronization, it is still a major contributor to impurity radiation in VH–mode discharges [13]. Future experiments are planned to further reduce oxygen by performing boronization between discharges and to assess the relevance of VH–mode for the next generation of fusion devices.

This work was supported by the U.S. Department of Energy under Contract No. DE-AC03-89ER51114.

REFERENCES

[1] J. Winter, H.G. Esser, L. Koenen, et al., J. Nucl. Mater. **162-164**, (1989) 713.

[2] T . Hodapp, G.L. Jackson, J. Phillips, et al., Proceedings of the 14th Symposium on Fusion Engineering, September 30-October 4,1991, San Diego, California, 1991 (to be published, IEEE, New York).

[3] J. Phillips, T . Hodapp, K. Holtrop, et al., to be published in J. Vac. Sci. Technol. A (1992).

[4] G.L. Jackson, J. Winter, T .S. Taylor, et al., Phys. Rev. Lett. **67** (1991) 3098.

[5] P .N. Yushmanov, T . Takizuka, K.S. Riedel, et al., Nucl. Fusion **30**, (1990) 1999.

[6] D.P . Schissel, J.C. DeBoo, K.H. Burrell, et al, Nucl. Fusion **31** (1991) 73.

[7] J. Winter, private communication (1991).

[8] W .P . West, N.H. Brooks, S.I. Lippmann, et al., Bull. Am. Phys. Soc. **36** (1991) 2476.

[9] G.L. Jackson, J. Winter, S.I. Lippmann, et al., J. Nucl. Mater. **185** (1991) 139.

[10] G.L. Jackson, and the DIII–D Team, J. Vac. Sci. and Technol. A, to be published (1992).

[11] G.L. Jackson, J. Winter, T .S. Taylor, et al., Phys. Fluids B, to be published (1992).

[12] G.L. Jackson, T .S. Taylor, and P .L. Taylor, Nucl. Fusion **30**, 2305 (1990).

[13] S.I. Lippmann, et al., this conference.

DATE
FILMED
8/25/92